Monatsh Chem (2011) 142:997–1003
DOI 10.1007/s00706-011-0591-6

ORIGINAL PAPER

A sharp J-band-like electronic absorption peak observed for the chromonic liquid crystal of bisazo dye Ponceau SS in water

Michio Kobayashi · Shin-ichi Komiya · Toshiaki Maruyama · Yasuhiro Kasahara · Toshihiko Hoshi

Received: 3 August 2010 / Accepted: 15 July 2011 / Published online: 24 August 2011

Abstract The bisazo dye Ponceau SS forms an acute oblique (V-type) dimer in dilute aqueous solution. In concentrated aqueous solution, these V-type dimers are considered to stack to form V-type blocks of chromonic liquid-crystalline (LC) columns. The weak interactions among these LC columnar V-type blocks have been spectroscopically investigated. On increasing the concentration of Ponceau SS at 25 °C, the V-type LC columnar blocks form a rhombus-type LC columnar block at 2 wt% concentration. These rhombus-type LC columnar blocks are further aligned at an acute angle at 5 and 10 wt% concentrations. The rapidly cooled 10 wt% LC sample shows an unusually sharp J-band-like peak in the electronic absorption spectrum. The emergence of this J-band-like peak has been analyzed from the viewpoint of an exciton model, suggesting that many nearest neighbor unique molecules belonging to many different rhombus-type LC columnar blocks are aligned in a head-to-tail manner to give a giant quasi-linear head-to-tail-type exciton.

Keywords UV/Vis spectroscopy · Aggregation · Dyes · Chromonic liquid-crystalline column · J-band

M. Kobayashi (✉) · Y. Kasahara · T. Hoshi
Department of Chemistry and Biological Science, College of Science and Engineering, Aoyama Gakuin University, Sagamihara, Kanagawa 252-5258, Japan
e-mail: michio@chem.aoyama.ac.jp

S. Komiya · T. Maruyama
Department of Chemistry, Technological University of Nagaoka, Nagaoka, Niigata 940-2188, Japan

Introduction

Conventional amphiphiles form lyotropic liquid crystals (LCs) through the so-called hydrophobic effect. The formation of this kind of LC is known to be endothermic and to be driven by an increase in entropy of the water molecules surrounding the LC domain [1, 2]. On the other hand, chromonic mesogens form exothermically lyotropic LCs through self-association among mesogen molecules [2]. In the chromonic LCs, which emerge in higher-concentrated aqueous solutions of some aromatic compounds having no hydrophobic long alkyl chain, the constituent molecules associate via dispersion forces to form LC columns that are characteristically arranged as a result of weak interactions among LC columns [3–7]. Some models were proposed for the arrangement of these LC columns in the LC phase on the bases of NMR, X-ray diffraction, FT-IR, and optical microscopy studies [8–15]. However, few studies have been performed on the electronic absorption spectra of chromonic LCs except the work by Harrison et al. [16], Ruslim et al. [17], and Collings et al. [18–21]. Harrison et al. [16] found that the onset of J-aggregate formation for cyanine dyes is practically concomitant with the occurrence of mesophases. They also pointed out that further studies are necessary to distinguish between J-aggregate and mesophase formations. Ruslim et al. [17] described that H-like aggregates are formed in the LC phase of Direct Blue 67 along with J-like or H-like aggregates with different slippage angles. Collings et al. [18–21] found, using an exciton model for the excitonic interactions within the single LC column, that the absorption coefficient decreases as the number of molecules in an LC column increases, and estimated the stacking free energy change for the LC column formation.

In the present study, the electronic absorption spectral changes on the phase transition of the chromonic LC of the

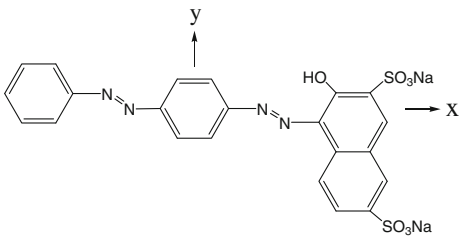

Fig. 1 Molecular structure of PSS

bisazo dye Ponceau SS (PSS, 3-hydroxy-4-[2-[4-(2-phenyldiazenyl)phenyl]diazenyl]-2,7-naphthalenedisulfonic acid disodium salt, Fig. 1) in water were studied to investigate the intermolecular and inter-LC-columnar weak interactions in these chromonic LCs and to obtain spectroscopic information regarding the arrangement of the chromonic LC columns.

Results and discussion

The concentration dependence of the electronic absorption spectra of PSS in dilute (1.0×10^{-5}–1.0×10^{-2} mol dm^{-3}) aqueous solutions is shown in Fig. 2.

On increasing the concentrations, the spectra are changed with isosbestic points, implying that monomer and dimer of PSS are equilibrated in this concentration range. The monomer's first band (600–450 nm) peaking at 520 nm is split into two bands on dimer formation, the main band occurring at 510 nm and a shoulder at around 560 nm. The exciton-splitting model to be considered later suggests that the aforementioned dimer adopts an oblique arrangement with an acute angle (cf. Fig. 7) between the two monomers' first electronic transition moments [22]. In order to know the geometrical structure of the dimer, it is very important to elucidate the polarization of each electronic transition band. Thus, the polarization spectrum of PSS was measured in a stretched polyvinyl alcohol (PVA) film (Fig. 3).

The absorption spectrum ($D_{//}$ spectrum) shows that three bands apparently exist at 528.5, 360, and 245 nm. The sample molecules in a stretched polymer (PVA) film are oriented with their longer molecular axes approximately parallel to the stretching direction of the film. This means that electronic transition bands with larger and smaller Rd values are polarized along longer and shorter (or out-of-plane) molecular axes, respectively. It is thus found that the 528.5 and 360 nm bands with larger Rd values are longer-axis (L) polarized, and the 245 nm band with smaller Rd values is shorter-axis (S) polarized. Inspecting in detail the Rd spectrum, weak electronic bands with minima or smaller Rd values are recognized at ~400, ~320, and

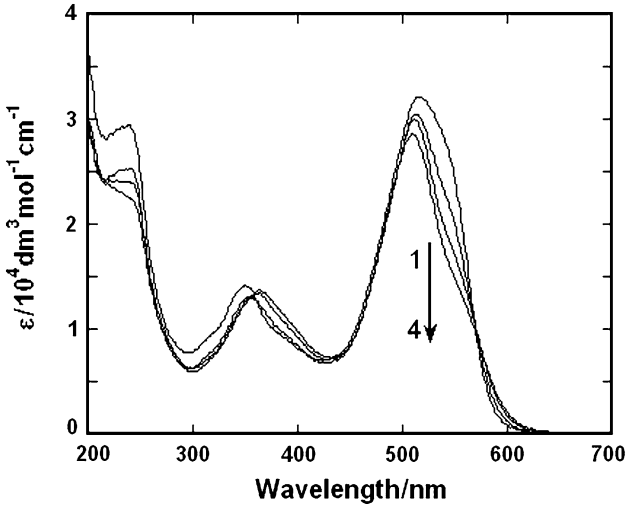

Fig. 2 Concentration dependence of electronic absorption spectra of PSS in dilute aqueous solutions: *1* 1.0×10^{-5}, *2* 1.0×10^{-4}, *3* 1.0×10^{-3}, *4* 1.0×10^{-2} mol dm^{-3}

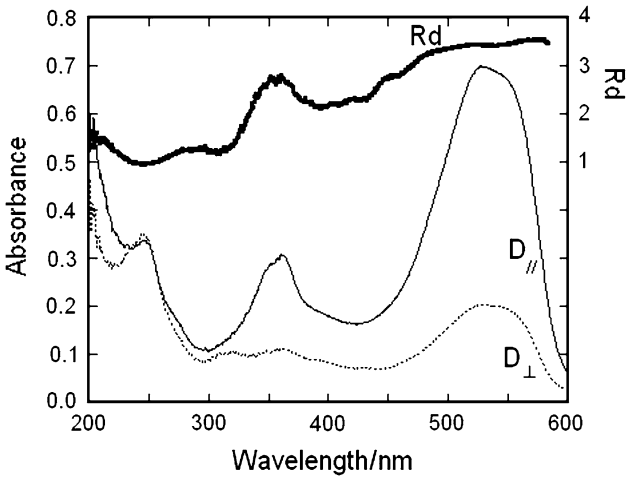

Fig. 3 The polarized absorption spectrum of PSS in the stretched PVA film

275 nm, which are polarized along the shorter molecular axis. These observations are compared with molecular orbital (MO) calculated results for the $\pi\pi^*$ electronic transitions in Table 1.

The calculated results correspond well to the observed ones except the ~400 nm observed band. That is, the observed 528.5, 360, ~320, 275, and 245 nm bands are safely assigned to the calculated transitions $\pi\pi_1^*$, $\pi\pi_2^*$, $\pi\pi_6^*$, $\pi\pi_9^*$, and $\pi\pi_{15}^*$, respectively. The transition moment directions of the calculated $\pi\pi_1^*$ (−12.5°) and $\pi\pi_2^*$ (−30.2°) transitions are almost along the longer molecular axis in accordance with the observed polarizations. The angles in parentheses are the transition moment directions calculated with respect to the *x*-axis of the PSS molecule (cf. the molecular structure given in Fig. 1). The

Table 1 Comparison of observed and calculated electronic transitions of PSS

	Wavelength/nm		Intensity		Polarization direction	
	Calc	Obs	Calc[a]	Obs[b]	Calc[c]	Obs[d]
$\pi\pi_1^*$	508.3	528.5	1.688	1	−12.5°	L
$n\pi^*$		~400				S
$\pi\pi_2^*$	371.4	360	0.230	0.45	−30.2°	L
$\pi\pi_3^*$	347.3	~350	0.040	0.07	73.4°	S
$\pi\pi_5^*$	334.4		0.035		3.6°	
$\pi\pi_6^*$	322.6	~320	0.014	0.08	−82.0°	S
$\pi\pi_9^*$	280.3	275	0.209	~0.1	82.4°	S
$\pi\pi_{12}^*$	253.3		0.189		−81.2°	
$\pi\pi_{14}^*$	248.4		0.165		−88.3°	
$\pi\pi_{15}^*$	245.0	245	0.728	0.52	−82.4°	S

[a] Oscillator strength

[b] Relative intensity

[c] The angles against the *x*-axis (cf. the molecular structure of PSS given in the text)

[d] L and S mean longer and shorter molecular axes, respectively

transition moment directions of the calculated $\pi\pi_6^*$ (−82.0°), $\pi\pi_9^*$ (82.4°), and $\pi\pi_{15}^*$ (−82.4°) transitions also reproduce well the observed shorter-axis polarizations for ~320, 275, and 245 nm bands. The $\pi\pi_3^*$ transition may appear as a shoulder at around 350 nm. The ~400 nm band is considered, since no $\pi\pi^*$ transition is computed in this wavelength region, to be assigned to the out-of-plane polarized $n\pi^*$ electronic transition related to azo groups. Since the first electronic transition of PSS is proved, as described above, to be polarized along the longer molecular axis, the longer molecular axes of the two monomers are considered to be arranged obliquely with an acute angle in the dimer formed in the dilute aqueous solution.

Figures 4, 5, and 6 show electronic absorption spectra measured at 25 and 75 °C for the PSS–water system, whose concentrations are 2.0, 5.0, and 10.0 wt%, respectively.

In the present experiments, the LC samples were prepared by standard and nonstandard methods. The former method is described in the "Experimental" section. In the nonstandard method, the LC samples prepared by the standard method were soaked in liquid nitrogen and then warmed to room temperature. The nonstandard sample is not in LC phase but in the microcrystalline state in which the intermolecular interaction in the LC phase is considered to be emphasized. The electronic absorption spectra of the standard and nonstandard samples are given in parts a and b in each figure (Figs. 4, 5, 6), respectively. According to Fig. 5a for the standard 5 wt% sample, the first band (700–450 nm) measured at 75 °C is greatly changed in shape by lowering the temperature to 25 °C, i.e., the

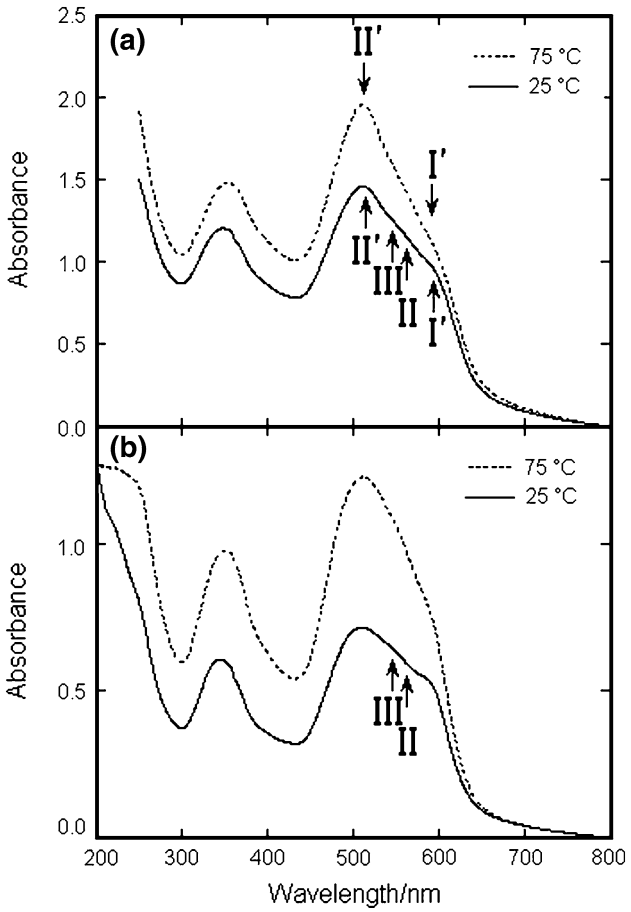

Fig. 4 Electronic absorption spectra of 2.0 wt% PSS/water LCs prepared by the standard (**a**) and nonstandard (**b**) methods

relative intensity of the 600 nm band (band I′) with respect to the 509 nm shoulder band (band II′) at 75 °C is greatly increased at 25 °C. This means that the weak intermolecular or inter-LC-columnar interactions become more prominent by lowering the temperature. Two electronic bands are obviously recognized at 600 (band I) and 500 (band IV) nm at 25 °C. Furthermore, at 25 °C one or two additional bands (band II and/or III) are considered to exist between the bands I and IV. Here, it should be noted that because bands II and III evidently exist in Fig. 6, as discussed below, these bands are safely considered to emerge in Figs. 5 and 4, too. Polarization microscopy shows that the PSS aqueous solutions used in the present experiments are isotropic at 75 °C and in an anisotropic chromonic LC phase at 25 °C. Although the solution shows isotropic properties at 75 °C, PSS molecules exist as aggregate at 75 °C, because the first band is split into two bands I′ and II′ (Fig. 5a) similar to the spectrum of the 10^{-2} mol dm^{-3} solution shown in Fig. 2. When the concentration of PSS is decreased to 2 wt%, the bands I′ and II′ are still observed at 75 °C (Fig. 4a). On lowering the temperature to 25 °C, the bands II and III emerge along with the bands I′ and II′ but

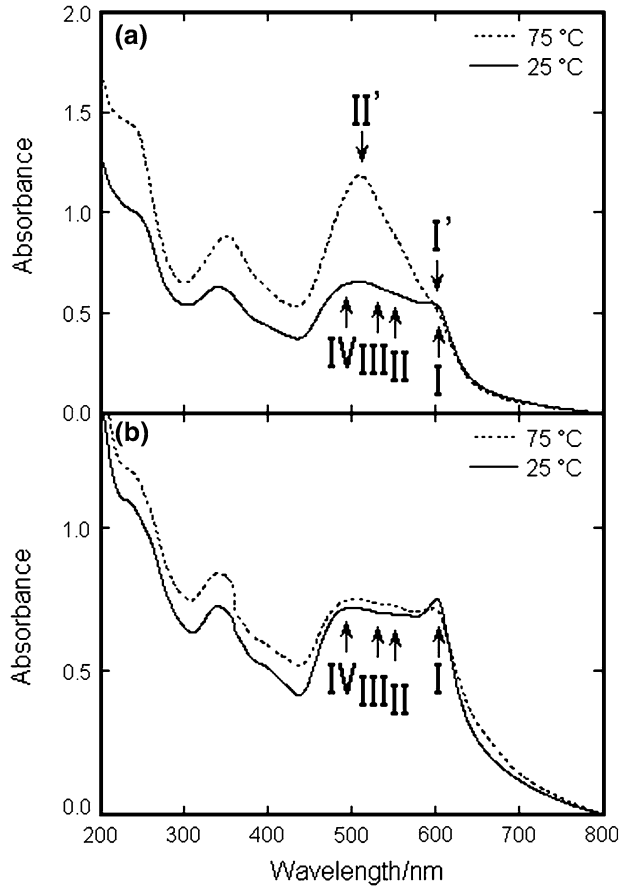

Fig. 5 Electronic absorption spectra of 5.0 wt% PSS/water LCs prepared by the standard (**a**) and nonstandard (**b**) methods

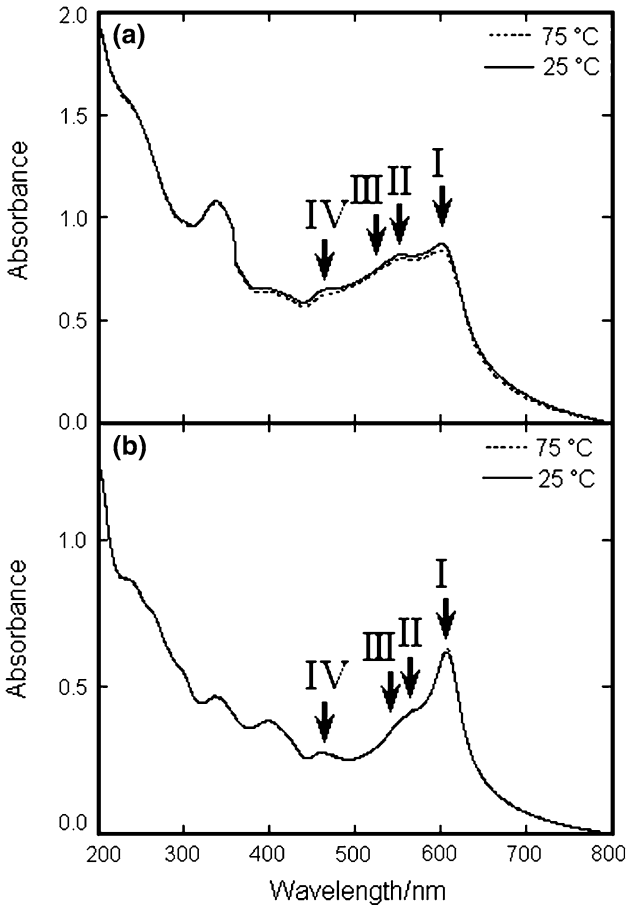

Fig. 6 Electronic absorption spectra of 10.0 wt% PSS/water LCs prepared by the standard (**a**) and nonstandard (**b**) methods

the bands I and IV are hardly recognized for the standard 2 wt% sample (Fig. 4a).

According to Fig. 5b, the nonstandard 5 wt% sample at 25 °C shows a distinct band peak at 601.5 nm and a broad band at 500 nm corresponding to the bands I and IV, respectively. The band I is unusually sharp given that the sample is highly concentrated (5 wt%) and that in the microcrystalline state, this usually inducing band broadening. This unusually sharp band is considered to be induced by the cooling process in the nonstandard method, and to sensitively reflect the intermolecular interaction which is peculiar to the chromonic LC phase and emphasized in the microcrystalline state. The spectrum is almost unchanged on raising the temperature from 25 to 75 °C, except that band I is broadened. In contrast, the cooling process in the nonstandard 2 wt% sample does not induce such an unusually sharp band peak as in the case of the 5.0 wt% sample (Figs. 4b and 5b). However, it seems that bands II and III are rather more clearly recognized on cooling (Fig. 4b). On increasing the concentration up to 10.0 wt%, all four bands I, II, III, and IV are clearly observed, and band I has a maximum intensity in the first band region (700–450 nm) although almost no temperature dependence is recognized for the spectrum of the standard sample (Fig. 6a). For the nonstandard 10 wt% sample, the spectrum measured at 25 °C coincides with that measured at 75 °C (Fig. 6b). It is noteworthy that the band I for the standard 10.0 wt% sample (Fig. 6a) is much intensified and unusually sharpened with a slight redshift for the nonstandard 10.0 wt% sample (Fig. 6b).

As seen from Fig. 5a, the spectrum of the standard 5.0 wt% sample is greatly changed on the phase transition from isotropic phase (75 °C) to liquid crystalline phase (25 °C). This spectral change is considered to be induced by the change in short/long-range interactions between/among LC columns. Furthermore, the influence of the interactions among LC columns on the chromonic LC spectra is qualitatively analyzed by considering the exciton interactions among LC columns. These exciton interactions are considered to arise from the interactions among the molecular excitons localized on the nearest neighbor unique molecules, which belong to different LC columns, to generate an extended exciton delocalized over two or more LC columns. The electronic transition from the

ground state to this extended exciton state generates the interactions among the molecular transition moments specified for the unique molecules mentioned above. These interactions provide an explanation for the spectral change caused by the exciton interactions among LC columns. The above spectral changes on the isotropic to LC phase transition cannot be explained by the model proposed by Attwood and Lydon [9] for the LC columnar arrangement. Since, in their model, the two nearest neighbor LC columns are perpendicularly arranged with T-type, the inter-LC-columnar exciton interactions are considered to be negligibly small. Thus, the molecular exciton interaction model, i.e., the molecular transition moment interaction model, which is applicable to the analysis of the present chromonic LC spectra of PSS, is proposed as shown in Fig. 7. In this figure the fine arrows represent the molecular transition moment for the long-axis-polarized first $\pi\pi^*$ transition band of PSS. Since PSS forms an oblique-type dimer in a dilute aqueous solution, the bands I′ and II′ observed in the isotropic phase (75 °C) are considered to be split due to an oblique-dimer-type (V-type) exciton interaction between two nearest neighbor unique molecules belonging to different LC columns to generate an extended V-type exciton (Fig. 7). Therefore, the bands I′ and II′ are assigned to the V-type LC columnar block structure (Fig. 8a), the angle made by two columns being acute. It is thus implied that the V-type LC columnar block structure survives mainly in the isotropic phase to generate the short-range intercolumnar interaction alone.

In Fig. 7 the molecular exciton interaction models are also shown for three possible types of tetramers formed from two oblique dimers, i.e., for head-to-tail, parallel, and oblique tetramers. In this figure, four exciton states (ψ_{I}, ψ_{II}, ψ_{III}, and ψ_{IV}) can be derived from four combinations of the monomer transition moments for each type of tetramer. For the head-to-tail tetramer, the transitions (represented by bold arrows) from the ground state to the exciton states of ψ_{I} with lowest transition energy and ψ_{IV} with highest transition energy are allowed, and those to ψ_{II} and ψ_{III} are forbidden. For the parallel tetramer, the transitions to ψ_{II} and ψ_{IV} are allowed, those to ψ_{I} and ψ_{III} being forbidden. For the oblique tetramer, the transitions to ψ_{II} and ψ_{III} are allowed, those to ψ_{I} and ψ_{IV} being forbidden. The two bands II and III newly observed in the LC phase have emerged between the bands I′ and II′ observed in the isotropic phase (Fig. 5a). This observation is in accordance with the exciton states for the oblique tetramer shown in Fig. 7. Thus, the bands II and III are assigned to the excitations from the ground to exciton states of ψ_{II} and ψ_{III} for the oblique tetramer, respectively. According to this exciton analysis, the bands II and III are considered to reflect an oblique-tetramer-type (rhombus-type) exciton interaction between two extended V-type excitons

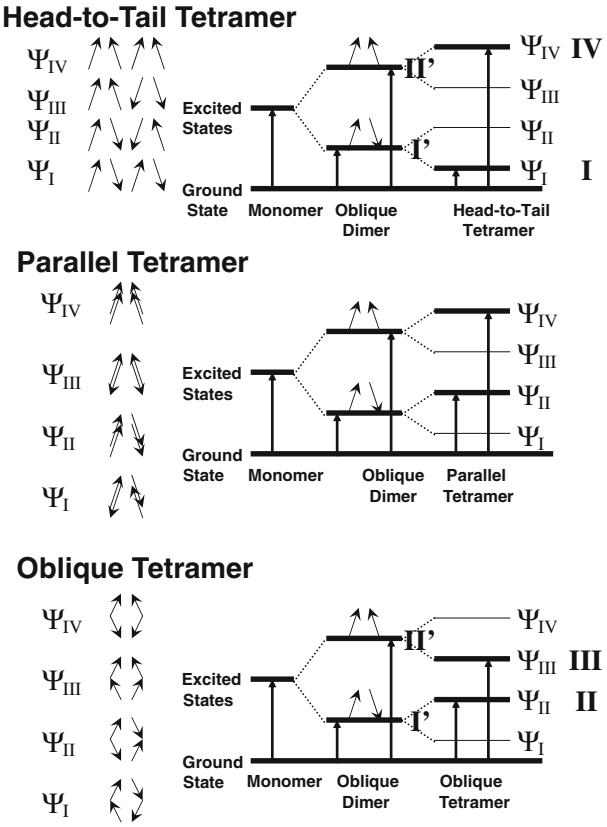

Fig. 7 Exciton interaction models for three types of tetramers formed from two oblique dimers: I, II, III, and IV represent the bands observed for PSS/water chromonic LC at 25 °C; I′ and II′ those for standard 2.0 and 5.0 wt% PSS/water isotropic phase at 75 °C

localized on two V-type LC columnar block structures to generate an extended rhombus-type exciton, and are assigned to a rhombus-type LC columnar block structure (Fig. 8b). On the other hand, the band IV in the LC phase is located on the higher energy side of the band II′ in the isotropic phase and the band I is on the slightly lower energy side of the band I′ (Fig. 5a).

This spectral behavior can be explained by the molecular exciton interaction model for the head-to-tail-type tetramer shown in Fig. 7. Here, it should be pointed out that the emergences of the bands II and III precede those of the bands I and IV with increasing concentrations of PSS. That is, the bands II and III appear at lower concentrations than the bands I and IV do, implying that the formation of the rhombus-type LC columnar blocks immediately follows that of V-type LC columnar blocks. Thus, the bands I and IV are considered to reflect a head-to-tail-type exciton interaction between/among extended rhombus-type excitons localized on rhombus-type LC columnar blocks to generate an extended head-to-tail type exciton. Therefore, the bands I and IV are assigned to a head-to-tail-type arrangement of rhombus-type LC columnar blocks

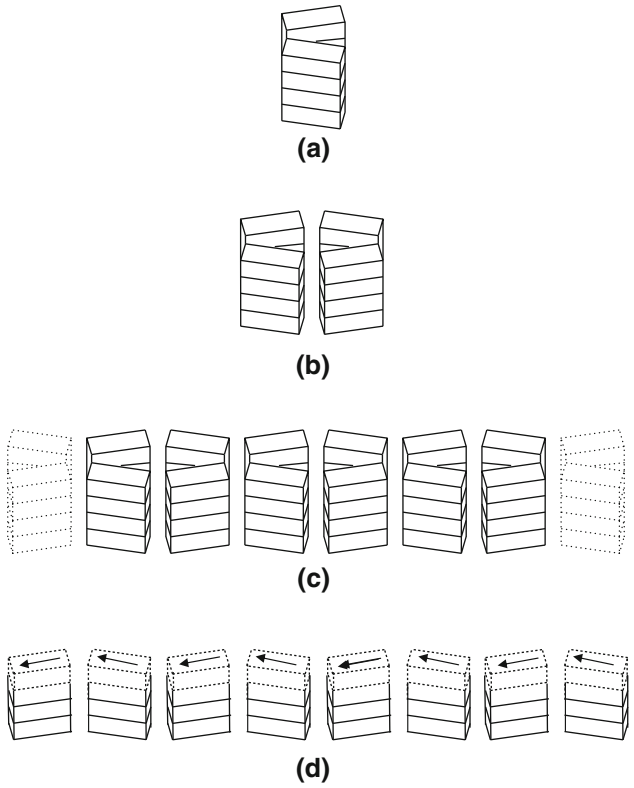

Fig. 8 LC columnar arrangements for the PSS/water chromonic LCs suggested by the present exciton model analysis: **a** V-type LC columnar block, **b** rhombus-type LC columnar block, **c** head-to-tail type arrangement of rhombus-type LC columnar blocks, **d** long-range quasi-linear head-to-tail arrangement of molecular transition moments specified for the nearest neighbor unique molecules shown by the cuboids represented by *dotted lines*

(Fig. 8c). As already noted, there is a marked tendency for the band I to be intensified and sharpened on increasing concentrations and on microcrystallizing by means of the nonstandard method, resulting in band I being far more intense than the band IV and the former band changing into a J-band-like sharp band (Fig. 6b). This marked spectral characteristic originates from a middle- or long-range head-to-tail-type exciton interaction among several or many rhombus-type LC columnar blocks which are aligned at an acute angle (Fig. 8c). When many rhombus-type LC columnar blocks are aligned at an acute angle, a long-range quasi-linear head-to-tail arrangement of LC columns appears, as shown in Fig. 8d. Thus, the molecular exciton interaction along this arrangement produces a giant quasi-linear head-to-tail-type transition moment specified for the nearest neighbor unique molecules represented by the dotted cuboids in Fig. 8d. This giant transition moment is considered to give rise to a so-called J-band, which corresponds to the sharp band I in Fig. 6b, along with the weak band IV. In Fig. 5a for 25 °C and in Fig. 5b for 25 and 75 °C, the aforementioned spectral feature, i.e., that the band I is more intense than band IV, is considered to be obscured by an overlap of the bands I′ and II′. This implies that the V- and rhombus-type LC columnar blocks coexist in the LC and cooled microcrystalline phases for 5 wt% sample of PSS.

Experimental

Commercially available PSS (Aldrich) was purified as follows: crude PSS was dissolved in *N*,*N*-dimethylformamide (DMF) and filtered to remove insoluble impurities. Acetone was added to the filtrate and reddish violet crystallites were obtained after standing overnight. The PSS crystallites thus purified were dissolved in an appropriate amount of water in V-vials, the solutions obtained being aged overnight at 80 °C to get LC samples of 2, 5, and 10 wt% concentrations. These LC samples were sandwiched between two quartz glass plates sealed with epoxy resin. The formation of LCs for 2, 5, and 10 wt% samples was confirmed by use of a polarizing microscope (Leica, DMLSP) attached to a CCD camera (Fuji film, HC-300Z). Electronic absorption spectra were measured with a Shimadzu UV-3100PC spectrophotometer. The polarization spectrum of PSS was measured by the stretched polymer film method [22]. In the figure of the polarization spectrum, the $D_{//}$ and $D_{\perp}$ are optical densities measured with polarized light beams whose electric vectors are parallel to and perpendicular to the stretching direction of the film, respectively. Dichroism ratio Rd is defined as $\mathrm{Rd} = D_{//}/D_{\perp}$.

For the MO calculation concerning the electronic transitions of the PSS molecule, a modified Pariser–Parr–Pople (PPP) method is adopted, in which resonance integrals between C–C, C–N, and C–O bonds are evaluated by the variable β method [23–25]. The resonance integrals between N–N bonds are fixed to −2.03 eV [26]. The valence state ionization potentials and electron affinities are taken as 11.22 and 0.62 eV for a carbon atom, 14.16 and 1.34 eV for an azo-nitrogen atom, and 33.00 and 11.47 eV for an hydroxyl oxygen atom [26]. The lone pair electrons on the azo groups are neglected. In the configuration interaction (CI) calculation, the one-electron excited configurations among the highest eight occupied and the lowest eight unoccupied orbitals are taken into account.

References

1. Atkins PW (1994) Physical chemistry, 5th edn. Oxford University Press, Oxford, p 973
2. Lydon JE (1998) Curr Opin Colloid Interface Sci 458:3
3. Hartshorne NH, Woodard GD (1973) Mol Cryst Liq Cryst 23:343
4. Attwood TK, Lydon JE (1984) Mol Cryst Liq Cryst 108:349

5. Perahia D, Luz Z, Wachtel EJ, Zimmermann H (1987) Liq Cryst 2:473
6. Jones F, Kent DR (1980) Dyes Pigm 1:39
7. Attwood TK, Lydon JE, Jones F (1986) Liq Cryst 1:499
8. Lydon JE (1980) Mol Cryst Liq Cryst 64:19
9. Attwood TK, Lydon JE (1986) Mol Cryst Liq Cryst Lett 4:9
10. Hui YW, Labes MM (1986) J Phys Chem 90:4064
11. Yu LJ, Saupe A (1982) Mol Cryst Liq Cryst 80:129
12. Goldfard D, Luz Z, Spielberg N, Zimmermann H (1985) Mol Cryst Liq Cryst 126:225
13. Lee H, Labes MM (1983) Mol Cryst Liq Cryst 91:53
14. Perahia D, Goldfarb D, Luz Z (1984) Mol Cryst Liq Cryst 108:107
15. Goldfard D, Labes MM, Luz Z, Poupko R (1982) Mol Cryst Liq Cryst 87:259
16. Harrison WJ, Mateer DL, Tiddy GJT (1996) J Phys Chem 100:2310
17. Ruslim C, Matsunaga D, Hashimoto M, Tamaki T, Ichimura K (2003) Langmuir 19:3686
18. Horowitz VR, Janowitz LA, Modic AL, Heiney PA, Collings PJ (2005) Phys Rev E 72:041710
19. Tomasik MR, Collings PJ (2008) J Phys Chem B 112:9883
20. Dickingson AJ, LaRacuente ND, McKitterick CB, Collings PJ (2009) Mol Cryst Liq Cryst 509:751
21. McKitterick CB, Erb-Satullo NL, LaRacuente ND, Dickingson AJ, Collings PJ (2010) J Phys Chem B 114:1888
22. Hoshi T, Tanizaki Y (1970) Z Phys Chem 71:230
23. Nishimoto K, Forster LS (1965) Theor Chim Acta 3:407
24. Nishimoto K, Forster LS (1966) Theor Chim Acta 4:155
25. Kobayashi M, Tanizaki Y, Hoshi T (1974) Can J Spec 19:3
26. Kumagai K, Hasegawa M, Enomoto S, Hoshi T (2001) Bull Chem Soc Jpn 74:441